2008 IEEE International Conference on
Robotics and Automation
Pasadena, CA, USA, May 19-23, 2008

Design and Motion Planning of a Two-Moduled Indoor Pipeline Inspection Robot

Young-Sik Kwon, Hoon Lim, Eui-Jung Jung, Byung-Ju Yi, *Member, IEEE*[1]

***Abstract*—This paper deals with design and motion planning of a reconfigurable robot that can be used for inspection of 80-100mm pipelines. This robot consists of two connecting modules and each module consists of three pairs of caterpillar, which is operated by micro DC motor. The robot is foldable by using an embedded four-bar mechanism and compression of a spring connected to the four-bar allows the robot to maintain contact with the wall of pipelines. Controlling the speed of each caterpillar independently provides a steering capability to go through elbow and T-branch. The robot system has been developed and the validity of this mechanism was proved by experimentation.**

I. Introduction

RECENTLY, many pipeline inspection robot systems have been developed. Initially, development of pipeline robot has started for inspecting large-sized pipelines ranging from 100 to 200mm, which are adequate to manufacturing sites. Recently, pipeline inspection robot systems smaller than 100mm pipeline have been of interest

Hirose [1] proposed several types of pipeline inspection robots ranging from Φ25, Φ50, up to Φ150 pipe. Horodinca [2] proposed simple types of pipeline inspection robots ranging from Φ40, Φ70, up to Φ170 pipe. Muramatsu [3] and Roh[4,9] investigated pipeline robots for underground urban to overcome the sharp curve inside the pipeline. Duran [5-6] developed an image processing algorithm to acquire the image of the pipeline by combining the image data of CCD camera and laser diode. Tao[7] developed pipeline inspection robots for detecting the defect of inner pipe. Jun and Jiang[8] proposed robot that has six wheeled driving arms fixed circumferentially with 60 degrees apart on the robot body frame. Moghaddam and Hadi[10] developed PIC(Pipe Inspection Crawler), which is a mobile robot for inspection pipelines with 10 to 20 inches diameter.

However, previously developed pipeline robot systems have been tested at straight or slightly inclined or simply curved pipelines. Navigation through a pipeline with multiple curves or T-branch is still a difficult problem. In this paper, we introduce a reconfigurable pipeline inspection robot designed for inspecting 80~100mm pipelines. This robot was designed to pass through multiple elbows or T-branch by collaboration of two robot modules connected by a compression spring. Controlling the speed of caterpillar independently provides a steering capability so that it can go through at elbow and T-Branch. A static force analysis was performed for actuator sizing. We show the validity of this robot system by experimentation.

Y. S. Kwon is with the School of Electrical Engineering and Computer Science, Hanyang University, Korea. (e-mail: yskwon80@gmail.com)

H. Lim with the School of Electrical Engineering and Computer Science, Hanyang University, Korea. (e-mail: yasu97@nate.com)

E. J. Jung is with the School of Electrical Engineering and Computer Science, Hanyang University, Korea. (e-mail: jeuij@yahoo.co.kr)

B. J. Yi is with the School of Electrical Engineering and Computer Science, Hanyang University, Korea. (corresponding author to provide phone: 82-31-400-5218; fax: 82-31-416-6416; e-mail: bj@hanyang.ac.kr)

II. Characteristics of Robot

A. Mechanism

The robot consists of a main body, three linkage structures, and caterpillar wheel parts as shown in Fig. 1. The length of robot is 70mm and the exterior diameter changes from 80mm up to 100mm. The main body contains the main board consisting of a micro controller (AVR, Atmega8) and a motor drive and sensor processor (AVR, Atmega128), and a linkage structure connects the main body to a caterpillar wheel part. Each caterpillar wheel contains a micro DC motor. The body is constructed as a triangular shape, which is adequate to support the three linkage structures. For each chain, two four-bar linkage structures similar to scissors are connected to the hinge joints grounded at the main body. And the hinges are connected by a spring-shaft. The deflection of the spring allows foldable characteristic of the linkage structure when the caterpillar wheel contacts the rough surface of the pipeline.

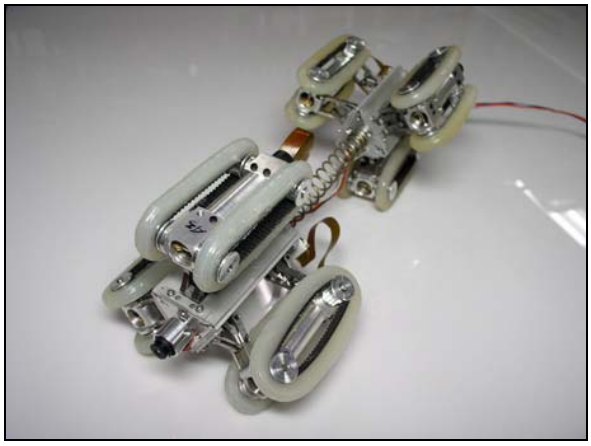

Fig. 1. Whole view of the pipeline inspection robot

A micro DC motor equipped with an encoder is enclosed inside the caterpillar wheel parts, and its length is 10mm. The

encoder plays the role of measuring the moving distance of the robot. In the wheel mechanism, the driving power is transmitted to the wheel by a set of a bevel gear, a pulley, and a belt as shown in Fig. 2. The robot mechanism consists of three pairs of caterpillar, which is operated by micro DC motor. Fig. 1 shows that the two robot modules are connected by a spring so that a smooth steering can be achieved at T-branches or elbows. Each sub-chain is designed so that it is foldable to fit into the size of pipeline.

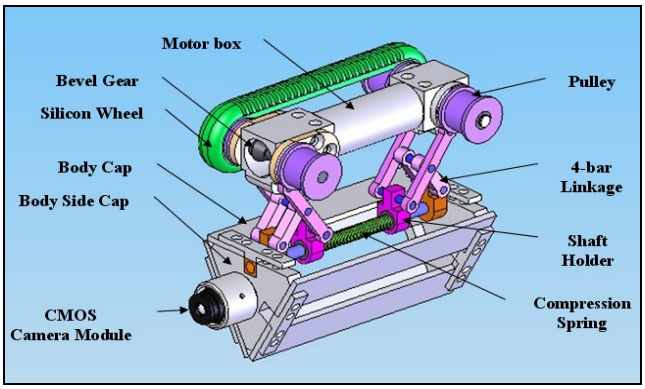

Fig. 2. Linkage structure and caterpillar wheel module

The caterpillar wheel of Fig. 3 is made of two gears and a wrapping Silicon belt. The Silicon plays the role of adhering to the wall since it has a very large friction coefficient.

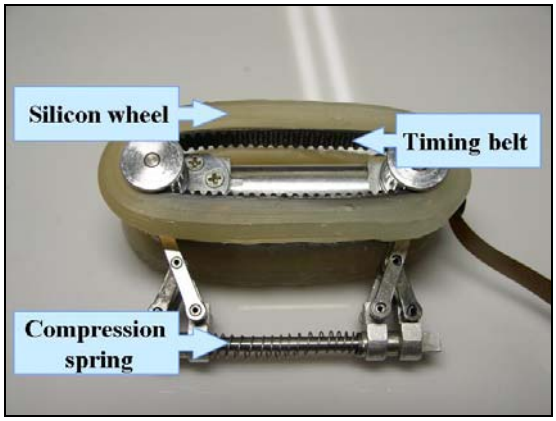

Fig. 3. Silicon caterpillar wheel

Each caterpillar wheel module is arranged 120 degrees apart. Thus, the robot is able to hold the surface of the pipeline firmly while moving on the surface of the pipeline very smoothly. Since each caterpillar is controlled independently, it is possible to perform steering at elbows or T-branches of pipelines by differentiating the velocities of the three wheels.

III. Analysis of Mechanism

A. Folding mechanism

The folding linkage structure can be represented as Fig. 4. This is a four-bar mechanism consisting of three revolute joins and one prismatic as depicted. Thus, the motion of all revolute joints can be described in terms of the displacement variable d_b.

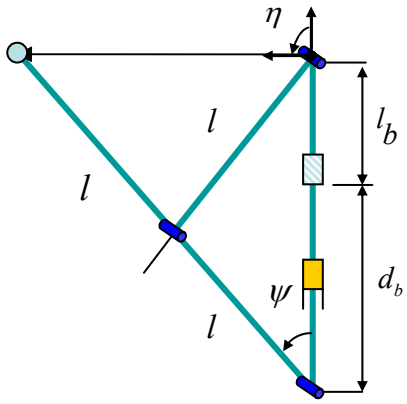

Fig. 4. Equivalent sub-chain : four-bar

B. Statics of mechanism

In order to decide the actuator size, it is necessary to perform the static analysis. In Fig. 5, F_{Cx} and F_{Cz}, respectively, denote the reaction force and the traction force exerted on the four-bar by the driving wheel. Only those forces conduct work. Applying the virtual work principle to the free-body diagram of Fig. 5 gives

$$\delta W = -F_{Cz}\delta z + F_{Bx}\delta x = 0, \quad (1)$$

where F_{Bx} is the compression force of the spring.

The corresponding displacements of those forces are expressed as

$$z = 2l\sin\psi, \quad x = 2l\cos\psi. \quad (2)$$

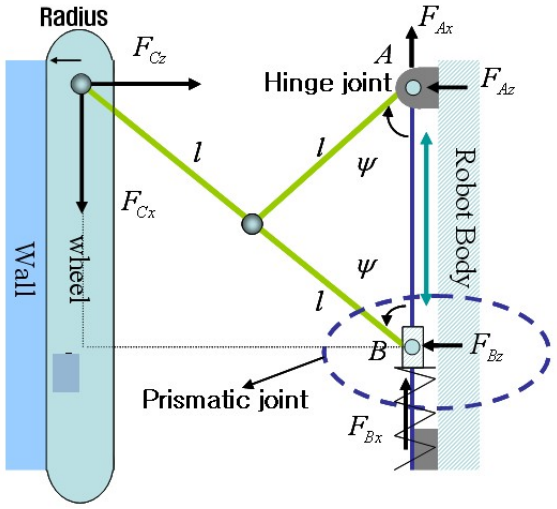

Fig. 5. Static analysis

Substituting (2) into (1) yields

$$\begin{aligned}\delta W &= -F_{Cz}\delta(-2l\sin\psi) + F_{Bx}\delta(2l\cos\psi) \\ &= F_{Cz}2l\cos\psi\delta\psi - F_{Bx}2l\sin\psi\delta\psi = 0.\end{aligned} \quad (3)$$

Rearranging (3) gives

$$F_{Bx} = F_{Cz}\frac{\cos\psi}{\sin\psi}. \quad (4)$$

Thus, the spring force at the prismatic joint B is related to the normal force F_{Cz} by

$$F_{Bx} = F_{Cz} \tan^{-1} \psi , \quad (5)$$

where $F_{Bx} = k\Delta x_{Bx}$.

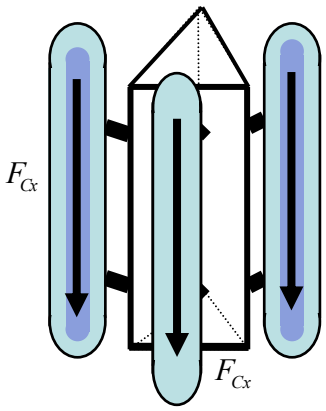

Fig. 6. Weight distribution

When the robot is moving vertically, the total weight W of the robot is the sum of the three traction forces exerted on the Silicon belt by the wall. Thus, each traction force F_{Cx} is one third of the whole weight of the robot structure. Thus, the size of the actuator enclosed in the wheel is calculated by

$$\tau = F_{Cx} r = \frac{Wr}{3}, \quad (6)$$

where r is the radius of the caterpillar wheel.

Applying the static force equilibrium for the foldable four-bar mechanism, we have

$$\sum F_z = F_{Cz} - F_{Az} - F_{Bz} = 0$$
$$\sum F_x = -F_{Cx} - F_{Bx} - F_{Ax} = 0. \quad (7)$$

Using Eq. (5) and Eq. (6), the reaction forces F_{Bz} and F_{Ax} are found as

$$F_{Bz} = \frac{W}{3} \tan\psi, \; F_{Ax} = \frac{W}{3} - F_{Cz} .$$

From the above static analysis, it is found that the reaction force F_{Cz} is supported by the spring force and that the large weight of the robot is structurally supported at the main body of the mechanism and does not influence the foldable motion of the linkage.

IV. Problem of One Module Experiment

A. Experimental Environment

We performed an experiment in an acrylic pipeline with the inside diameter of 90mm and the robot goes through a pipeline that possesses a cast iron elbow and a T-branch with the inside diameter of 80mm.

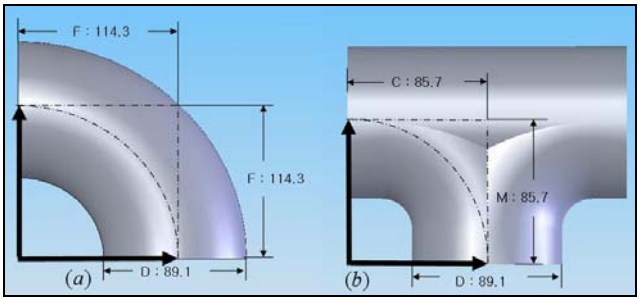

(a) iron Elbow (b)Cast iron T-branch

Fig. 7. Elbow and T-branch

The radius of curvature of the elbow is 114 mm and that of the T-branch is 86 mm as shown on Fig. 7. This pipeline is being used in standard pipes and it corresponds to the pipeline type 80 in Korea and Japan.

First of all, we check the motion capability at elbow and T-branch. At elbow, there are 3 types of motion and at T-branch 16 types. Table I shows the types of robot motion at elbow and T-branch.

TABLE I : Types of Motion

Pipe type	T-branch		Elbow
direction	Motion 1	Motion 2	
Horizontal ↓ Horizontal			
Horizontal ↓ Vertical			
Vertical ↓ Horizontal			
Vertical ↓ Manifold			

The experimental environment was constructed by assembling three T-branches and one elbow as shown in Fig. 8.

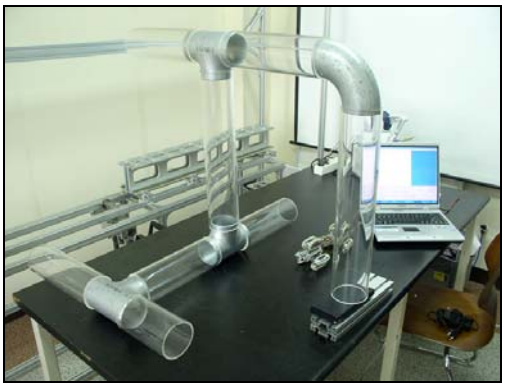

Fig. 8. Experimental Environment

B. *Analysis of Singular Motion*

When only one robot module is employed, sometimes it cannot go through the elbow as shown in Fig. 9(b). This case happens when the robot looses contact at the turning position. This case is called "motion singularity".

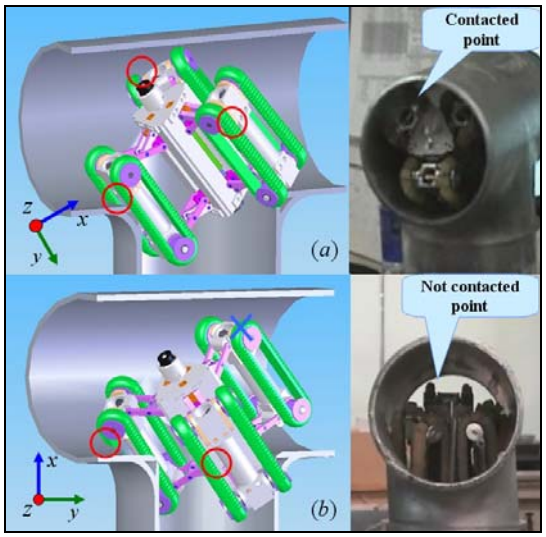

(a)Successful motion (b) Singular position
Fig. 9. Singularity problem

In the singular configuration of Fig. 9(b), any wheel chain is not able to contact the outer surface of the pipeline. On the other hand, the robot is able to turn if the inner caterpillar wheel contacting the corner maintains stationary and the two caterpillar wheels contacting the outer surface of the pipeline run.

To cope with such motion singularity problem, we employ collaboration of two robot modules as shown Fig. 10.

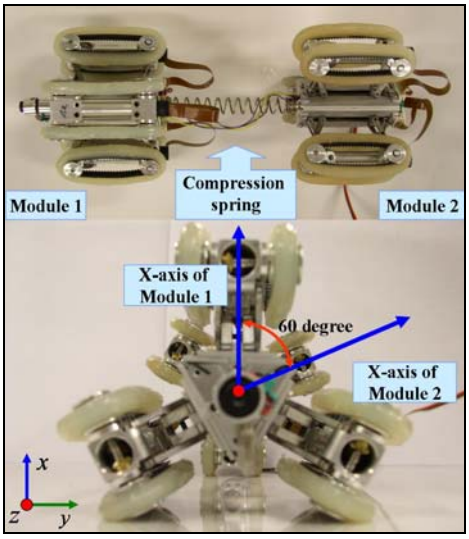

Fig. 10. Collaboration of two modules

The two modules are connected by a compression spring. The spring plays the role of smooth steering at elbow and T-branch. Fig. 10 also shows that the second module is rotated 60 degrees relative to the first module. This arrangement greatly helps avoiding motion singularity. Even though the first module confronts with motion singularity, the first module is able to pass through the elbow by the pushing force of the second module. On the other hand, if the first module is able to go through the elbow, the first module pulls the second module even though the motion singularity happens in the second module. Here, the pushing/pulling force generated by the compression spring helps successful steering at elbow or T-branch.

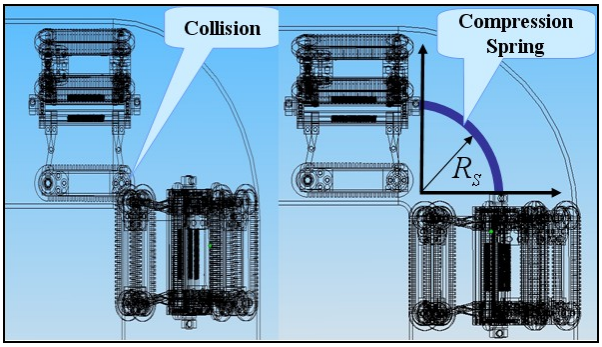

Fig.11. Co-work configuration

The length of the spring is chosen as follows. The minimum radius of curvature of the spring can be found by a geometric analysis of Fig. 11 such that the two modules do not interfere one to each other. Thus, the length of the spring is calculated as

$$L_s = 2\pi R_s \times (\theta/360) = 2\times 3.14\times 44\times 0.25 = 69mm \quad (7)$$

where θ denotes the angle change of the elbow. In practice, considering the amount of the spring compression, a spring of 80mm was employed. Table II shows the specification of the spring.

TABLE II : SPECIFICATION OF THE SPRING

Item		Value	Item		Value
Material	M	sus304	No. of active coils (turns)	Na	12
The modulus of elasticity (kgf/㎟)	G	7000	Total No. of coils (turns)	Nt	14
Wire diameter (mm)	d	1.3	Free length (mm)	Lf	85
Mean diameter (mm)	D	10.5	Spring constant	k	179.9
Compression Length (mm)	L	80	Compression load (g)	F	899.5

C. *Motion Planning Using Two Modules*

1) *Motion planning at elbow*

Fig. 12 shows the motion planning of the robot at elbow. In the straight path, the speed of the two robot modules is identical. Thus, the spring does not compress or elongate. However, if the front module enters the elbow, we plan the speed of the first module a little slower that that of the second module. Then, the spring is compressed. Resultantly, the

second module pushes the first module so that it can go though the elbow effectively. This really helps when the first module is located at a singular configuration. Similarly, when the second module goes though the elbow, we plan the speed of the first module faster than the second module. Then, the spring is elongated. Resultantly, the first module pulls the second module so that the second module can pass the elbow successfully.

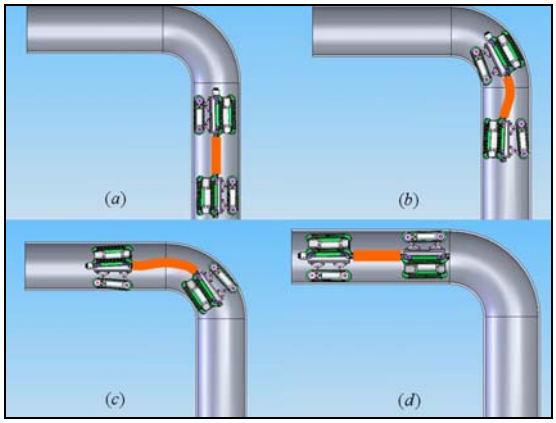

Fig.12. Motion planning at elbow

2) Motion planning at T-branch

Motion planning at T-branch is more complicate since there are many paths at T-branch. By experience, the transition from the horizon to the upward vertical pathway is found the most difficult task. This is because in this specific path of T-branch, there is not much area on which the wheels of the front module are able to step the wall of the pipeline. Also the direction of the gravity load hinders the rotation from the horizon to the upward vertical direction. Most previous pipeline robots have had such difficulty. However, the proposed robot system is able to overcome this difficulty by employing caterpillar wheel instead of rotating wheel, because the caterpillar wheel grasps relatively much contact area and the traction force of the silicon-covered wheel is also greater as compared to the usual rolling wheel having one point contact. Thus, the successive motion at T-branch can be generated as shown in (a) ~ (i) of Fig. 13.

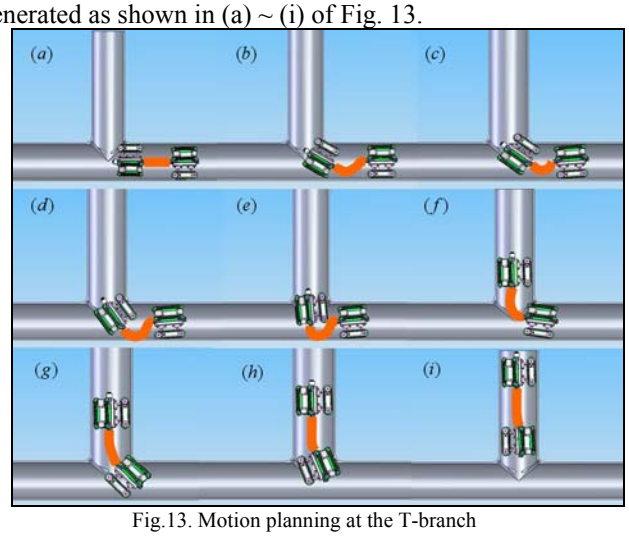

Fig.13. Motion planning at the T-branch

In Fig. 14, the circled parts denote the contact areas of the caterpillar wheels on the wall of the T-branch. This large contact area cannot be achieved by using a usual rotating wheel having only one point contact. To make a turn at the T-branch, the wheel contacting the inner corner remains stationary and the movement of the two outer wheels climbs up the wall of the T-branch toward the vertical pathway. After the front module enters the vertical pathway, the second module follows the front module because the spring guides the motion. In Fig. 13, In the process of (b) ~ (d), the compression force of the spring pushes the front module, and thus it assists the turning motion. In the process of (e) ~ (g), the front module pulls the following module so that it can go through the T-branch smoothly. Conclusively, the spring also plays an important role in the motion planning of the robot at T-branch.

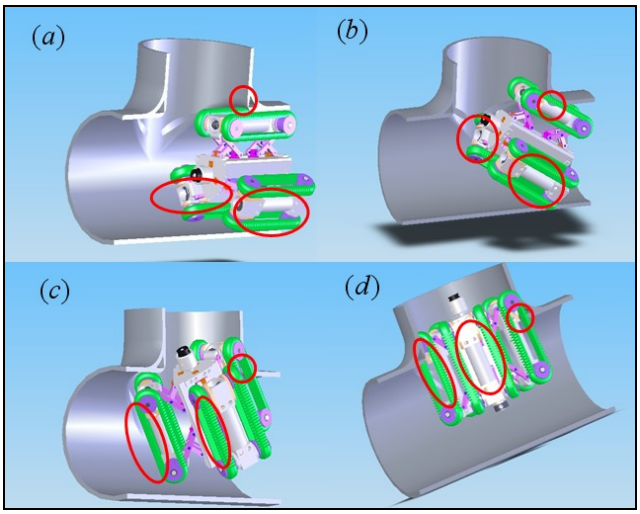

Fig.14. Contact configuration at T-branch

V. IMPLEMENTATION

A. Hardware

An effort was made to minimize the size of the robot system. A micro controller was designed small enough to install it inside the robot body. Also, a sensor unit that contains two accelerometers and one gyro sensor unit were designed for map building of pipelines. Encoders attached to the motors are also used to measure the displacement of the robot inside the pipeline.

Fig. 15 shows the system flow chart. When an order of the device control is given by PC's Graphic User Interface, it is transferred to the robot by a serial communication. Atmega8 controls motors and then Atmega128 demonstrates sensors' values after calculation.

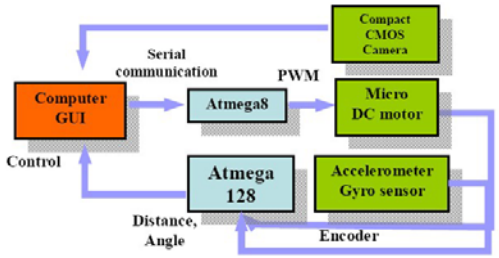

Fig. 15. System flow chart

Fig. 16 shows the entire picture of the pipeline inspection robot system. It is mainly divided into 4 parts ; a PC as a means of GUI and controlling the device, a robot-embedded part that contains many sensors and a processor for controlling the robot, a power link circuit storing communication module, and a grabber board that transfers the signal of a Micro CMOS camera to the PC.

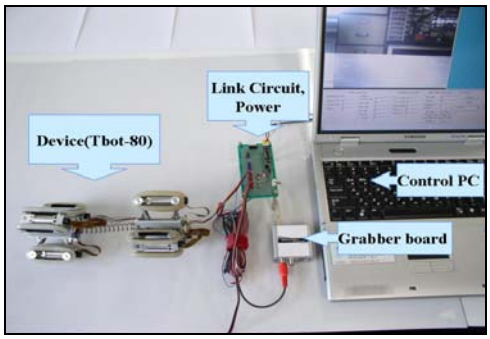

Fig. 16. Components of pipeline inspection robot

The robot control is completed by serial communication. When a motion command is given by the GUI control panel, Atmega8 controls the motor's speed by producing a PWM signal. It can control all of the Micro DC motors and measure the displacement of the robot by Encoder. All the motor drive and MCU are embedded in the main body of the robot as shown in Fig. 17.

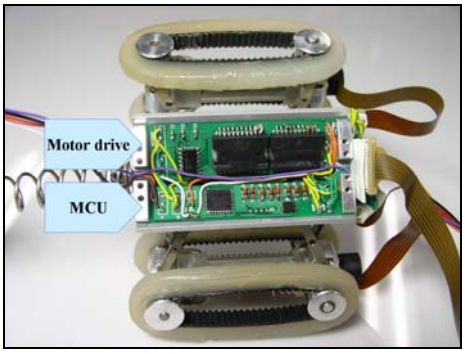

Fig. 17. Motor control module

Fig. 18 shows the minimized modularization of a Micro CMOS Camera and Sensors. The module that consists of a Micro CMOS Camera, a 2-axis accelerometer, a gyro sensor is 12mm in diameter and 20mm in length.

The view of the pipeline is provided to the user by using a Micro CMOS camera. This module makes it possible to inspect the condition inside the pipeline.

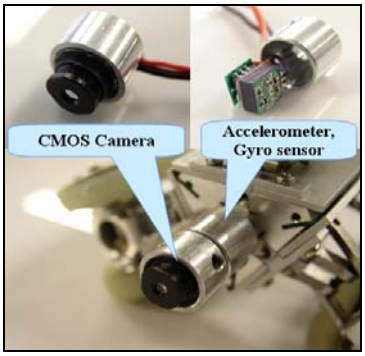

Fig. 18. Micro CMOS Camera and Sensors

Uses use the vision information at the GUI environment to control the robot. The 2-axis accelerometer is used to locate the robot with respect to the global reference coordinate while moving inside the pipeline, whereas the gyro sensor is used for measuring the rotation of the robot when it goes through a curved path.

Fig. 19 shows a sensor processor module where an Atmega128 is installed. The processor calculates the displacement and rotation of the robot by using the sensor signals from a 2-axis accelerometer, a gyro sensor, and an encoder of the micro DC motor. The measured values are transferred to the PC.

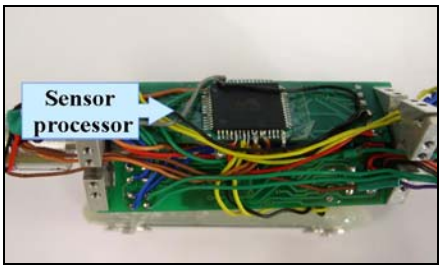

Fig. 19. Sensor process module

B. Graphic User Interface

We run the robot by using the GUI environment after opening a signal port. The GUI makes it possible to view the condition of the pipeline by using a micro CMOS camera and check how much the device has advanced from the global reference coordinate by using the encoder information of motors. Using the information of sensors, the map of the pipeline can be built as shown in Fig. 20.

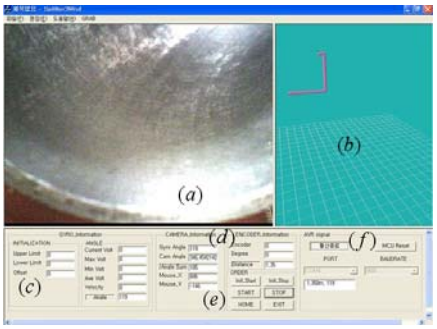

(a)Micro CMOS Camera view
(b)Map view
(c)Device orientation information
(d)Distance information
(e)Control button
(f)Serial communicate view

Fig. 20. Graphic User Interface

VI. Experimental Results

A pipeline consisting of 3 T-branches and 1 elbow was employed in experiment. TABLE III shows that the pipeline inspection robot is climbing up and down a vertical pipeline at the elbow. TABLE IV shows that the pipeline inspection robot is turning to several directions in a T-branch of the pipeline. The performance of the two-moduled pipeline inspection robot was verified through experimentation. The attached video clip shows the experimental result.

TABLE III : Type of Motion at Elbow

Direction	Motion
Vertical ⬇ Horizontal	
Horizontal ⬇ Vertical	

TABLE IV : Type of Motion at T-Branch

Direction	Motion
Horizontal ⬇ Vertical	
Horizontal ⬇ Horizontal	
Vertical ⬇ Horizontal	

VII. Conclusions

We developed a pipeline inspection robot that can be applied to inspection of 80~100mm pipeline. Using a two-moduled robot modules connected by a compressive spring, the turning motion at both elbow and T-branch can be conducted successively. Arrangement of the two modules by 60 degree's offset helps avoiding the singular motion. A caterpillar type wheel mechanism also assists to ensure enough contact area, specially in the T-branch. The performance of the proposed pipeline inspection robot system was verified through a variety of experiment under a test-bed environment.

Acknowledgment

This work was financially supported by MOCIE & ETEP (Electric Power Technology Evaluation & planning Center) through EIRC program, Republic of Korea. (I-2007-0-267-0-00)

References

[1] S. Hirose, H. Ohno, T. Mitsui, and K. Suyama, "Design of In-pipe Inspection Vehicles for Φ25, Φ50, Φ150 pipes," IEEE *International Conference on Robotics and Automation*, pp. 2309-2314, 1999.

[2] M. Horodinca, I. Doroftel, E. Mignon, and A. Preumont, "A simple architecture for in-pipe inspection robots," Int. Colloquium on Mobile and Autonomous Systems, 10 Years of the Fraunhofer IFF, Magdeburd, June 25-26,2002.

[3] M. Muramatsu, N. Namiki, R. Koyama, and Y. Suga, "Autonomous Mobile Robot in Pipe for Piping Operations," IEEE *International Conference on Intelligent Robots and Systems*, pp. 2166-2171, 2000.

[4] S.G. Roh, S.M. Ryew, J.H. Yang, and H.R Choi, "Actively Steerable Inpipe Inspection Robots for Underground Urban," IEEE *International Conference on Robotics & Automation*, pp. 761-766, 2001.

[5] O. Duran, K. Althoefer, and L.D. Seneviratne, "Automated Sewer Pipe Inspection through Image Processing," IEEE *International Conference on Robotics & Automation*, pp. 2551-2556, 2002.

[6] O. Duran, "Pipe Inspection Using a Laser-Based Transducer and Automated Analysis Techniques," *IEEE/ASME Transactions on Mechatronics*, Vol. 8, No. 3, pp. 401-409, 2003.

[7] J. Tao, Q. Peiwen, and T. Zhenqsu, "Development of magnetic flux leakage pipe inspection robot using Hall sensors", The 2004 international Symposium on Micro-Nanomechatronics and Human Science, pp. 325-329, 2004.

[8] C. Jun, Z. Deng, S.Y. Jiang, "Study of Locomotion Control Characteristics for Six Wheels Driven In-Pipe Robot", IEEE *International Conference on Robotics and Biomimetics*, pp. 119-124,2004.

[9] S.G. Roh and H.R. Choi, "Differential-drive in-pipe robot for moving inside urban gas pipelines", IEEE *Transactions on Robotics*, Vol. 21, No. 1. pp. 1-17, 2005.

[10] M.M. Moghaddam and A. Hadi, "Control and Guidance of a Pipe Inspection Crawler(PIC)", International Symposium on Automation and Robotics, pp. 11-14, 2005.